MAGNETIC RESONANCE IN MEDICINE **21**, 251–263 (1991)

Spoiling of Transverse Magnetization in Steady-State Sequences

Y. ZUR,*† M. L. WOOD,‡ AND L. J. NEURINGER*§

Francis Bitter National Magnet Laboratory, Massachusetts Institute of Technology, Cambridge, Massachusetts 02139; and ‡Department of Radiation Oncology, New England Medical Center and Tufts University, Boston, Massachusetts 02111

Received October 10, 1990; revised March 25, 1991

A detailed analysis is presented of a method to eliminate transverse magnetization prior to each rf excitation in pulse sequences with TR $< T_2$. It is shown that artifact-free images with high T_1 contrast can be obtained only if a phase shift that is incremented during each TR interval is applied to the transverse magnetization. Computer simulations are used to show that when this phase increment is 117°, the steady-state transverse magnetization prior to each rf pulse is nulled over a wide range of T_1, T_2, and rf tip angles, resulting in optimal T_1 contrast. Such nulling of steady-state transverse magnetization cannot be obtained by using large gradient pulses, or gradients of random or linearly incremented amplitude. Images of phantoms and human subjects confirm the theoretical predictions.

INTRODUCTION

Several imaging techniques have recently been proposed for the rapid acquisition of MR images, which employ gradient-refocused echoes and a short delay (TR) between successive rf pulses (*1–4*). In these sequences TR is kept shorter than T_2 and the magnetization is allowed to reach steady state. These techniques can be divided into two groups: (i) "refocused" steady-state sequences, where both longitudinal and transverse magnetization are allowed to reach steady state; (ii) "spoiled" steady-state sequences, where the transverse magnetization is made zero, or spoiled, prior to every rf pulse, so that only the longitudinal magnetization attains steady state.

The refocused steady-state sequences, referred to here as SSFP (*5, 6*), or steady-state free precession, provide images with a high signal-to-noise ratio, but with contrast that depends on T_1, T_2, TR, and the rf tip angle (*7*). These images do not provide the T_1 contrast available from partial saturation spin-echo sequences. The spoiled steady-state sequence, referred to here as FLASH (*1*) or fast low angle shot, gives images with good T_1 contrast and improved signal-to-noise ratio compared to T_1-weighted spin-echo sequences (*8*). Since TR $< T_2$, the transverse magnetization in an SSFP sequence does not decay to zero prior to each rf pulse in the train. Therefore, in order to obtain the good T_1 contrast available with FLASH sequences the transverse magnetization must be eliminated, or spoiled, prior to each of the rf pulses.

§ To whom reprint requests should be addressed.
† Present address: Elscint MRI Center, P.O. Box 550, Haifa, 31004, Israel.

0740-3194/91 $3.00

This paper presents a detailed theoretical analysis of a method for spoiling that was introduced earlier (*9, 10*). Computer simulations are performed and used to optimize the method. Images of phantoms and humans are presented which confirm the theoretical predictions. The method produces artifact-free images with completely spoiled transverse magnetization, even when TR $\ll T_2$. It is shown that spoiling with large gradients (*14*), gradient pulses of random or linearly incremented amplitude (*10–13*), or random phase shifts (*6*), is ineffective.

THEORY

In an SSFP pulse sequence, a train of rf pulses is applied to the spin system, with interpulse time interval TR shorter than T_2. The transverse magnetization of each isochromat acquires a phase shift of Φ radians during each TR interval, given by

$$\Phi = \int_0^{TR} \omega(t)dt, \qquad 0 \leq t \leq TR, \qquad [1]$$

where $\omega(t)$ is the resonance offset of the isochromat at time t. Magnetic field gradients and field inhomogeneities make the resonance offset depend on the spatial position of the isochromat, whereas Φ remains the same for all TR intervals.

Consider the train of rf pulses shown in Fig. 1. Immediately after the first rf pulse P_1, transverse magnetization S^+ is created. Since TR $< T_2$ this magnetization is refocused by subsequent rf pulses, such that a net transverse magnetization S^- appears prior to each rf pulse in the sequence. Approximately $3T_1$ s after the onset of the sequence, steady state is attained such that S^+ and S^- are the same for all rf pulses. These steady-state transverse magnetizations are denoted S^+_{ss} and S_{ss}, respectively, as shown in Fig. 1.

If the S_{ss} signal is eliminated ("spoiled"), then S^+_{ss} is equal to the steady-state transverse magnetization of the FLASH sequence, given by (*15*)

$$S^+_{FLASH} = M_0 \sin\alpha \left(\frac{1 - \exp(-TR/T_1)}{1 - \cos\alpha \cdot \exp(-TR/T_1)} \right), \qquad [2]$$

where α is the rf tip angle.

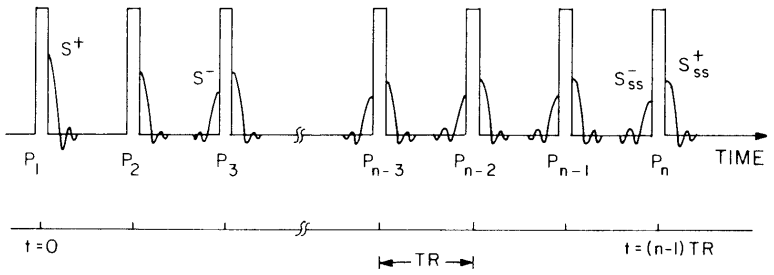

FIG. 1. A continuous train of rf pulses separated by the time interval TR, with TR $< T_2$. The transverse magnetization S^+, created by pulse P_1, is refocused by P_2 and appears prior to P_3 (denoted by S^-). After steady state is achieved, these two components are designated as S^+_{ss} and S_{ss}.

Time Evolution of a Single Isochromat

The time evolution of the phase of a *single isochromat* in an SSFP pulse sequence has been described previously (Ref. (*22*), Fig. A1). The amplitudes of the longitudinal and transverse components depend on (*16, 17*)

$$E_1 \equiv \exp(-\mathrm{TR}/T_1), \qquad [3a]$$

$$E_2 \equiv \exp(-\mathrm{TR}/T_2), \qquad [3b]$$

and on the rf tip angle (*18*).

Because of T_1 relaxation between the rf pulses, there is longitudinal magnetization prior to every rf pulse in the train. Therefore, the true situation is more complicated than indicated in Fig. A1 of Ref. (*22*). The total magnetization prior to any rf pulse in the train is, in fact, the sum of many magnetization components. Each one was created from longitudinal magnetization by some previous rf pulse, and has evolved through a unique trajectory. This is illustrated in Fig. 2 where the time evolution of the trajectories of three components prior to pulse P_n is shown. Component 1 in Fig. 2 is created from longitudinal magnetization by pulse P_{n-4}. Its phase is inverted by P_{n-2}, and prior to P_n it has zero phase. Components 2 and 3 are created by P_{n-3} and P_{n-2}, respectively. Prior to P_n, the phase of component 2 is zero, and the phase of component 3 is 2Φ. From Fig. A1 (Ref. *22*) and from this analysis, we see that when Φ is the same for all TR intervals, the phase of *all* magnetization components prior to any rf pulse is given by $k\Phi$, where k is an integer, i.e., $k = 0, \pm 1, \pm 2 \ldots$. After steady-state is attained, the magnetization becomes periodic in time, with period TR, and it is the same prior to any rf pulse.

Effect of Applied Gradients

Thus far, we have analyzed the time evolution of one isochromat subjected to a train of identical rf pulses. When magnetic field gradients are applied, the precession frequency of the spins becomes position-dependent. If the same gradient pulses are applied during each TR, and magnetic field inhomogeneities are neglected, the phase of a spin at position $\vec{r}$, is given by

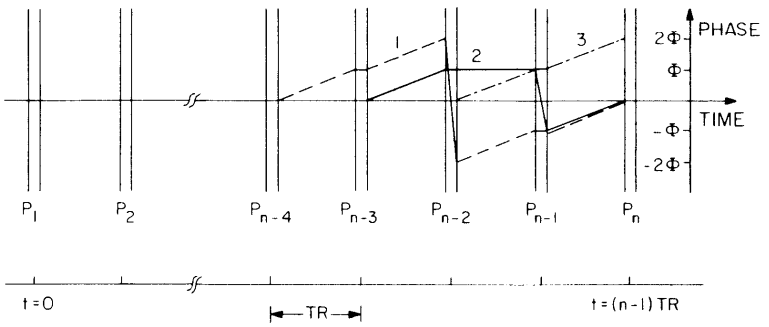

FIG. 2. An example of three magnetization components which evolve with different trajectories prior to pulse P_n. The phase accumulated between successive rf pulses is Φ.

$$\Phi(\mathbf{r}) = \gamma\mathbf{r} \cdot \int_0^{TR} \mathbf{G}(t)dt \equiv \gamma\mathbf{r} \cdot \mathbf{m}_0, \qquad [4a]$$

where

$$\mathbf{m}_0 \equiv \int_0^{TR} \mathbf{G}(t)dt, \qquad 0 \leq t \leq TR \qquad [4b]$$

and $\mathbf{G}(t)$ is the gradient applied at time t. The spin system now contains many different isochromats, each one with a different phase Φ. As shown above, the phases of all magnetization components prior to the rf pulses are $k \cdot \Phi(\mathbf{r})$, where k is an integer. If $\mathbf{m}_0$ is sufficiently large, magnetization components with nonzero phase will add destructively and cancel. Only magnetization components with zero phase prior to the rf pulse add coherently and contribute to the signal. In Fig. 2, magnetization components that evolve through trajectories 1 and 2 add coherently and contribute to the signal, but the component that evolves through trajectory 3 is dephased.

A Technique for Spoiling the Transverse Magnetization

As pointed out above, the transverse magnetization must be eliminated prior to every rf pulse in order to obtain the characteristic FLASH contrast. However, from the discussion in the preceding sections, it is seen that if Φ is the same for all TR and TR $< T_2$, this condition is not satisfied, even in the presence of magnetic field gradients.

This section shows how the transverse magnetization can be eliminated prior to any rf pulse by varying the phase Φ from one TR interval to another. Using this procedure, the phase of a given magnetization component will then depend on the trajectory through which it evolves. This is demonstrated in Fig. 3, where the magnetization trajectories 1, 2, and 3 of Fig. 2 are redrawn. The phase angle Φ now varies from one TR to another. The phase angle between rf pulses P_{n-4} and P_{n-3} is denoted $\Phi(n-4)$, the phase between P_{n-3} and P_{n-2} is $\Phi(n-3)$, and so on. Using this notation, the phases of the magnetization components evolving through trajectories 1, 2, and

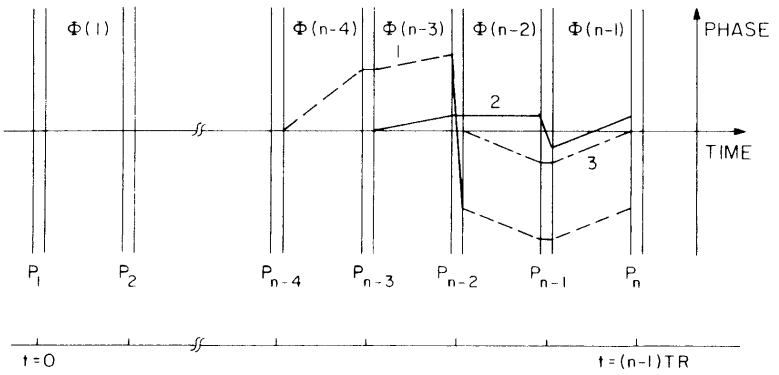

FIG. 3. The effect on the trajectories of Fig. 2 when the phase accumulated between any two consecutive rf pulses is not constant.

3 prior to rf pulse P_n are given by $\Phi(n-1)+\Phi(n-2)-\Phi(n-3)-\Phi(n-4)$, $\Phi(n-1)-\Phi(n-3)$, and $\Phi(n-2)+\Phi(n-1)$, respectively. By using this technique magnetization components that evolve through different trajectories acquire different phases, and their contributions may cancel each other, resulting in zero transverse magnetization prior to the rf pulse.

We denote the phase applied to the spins between the nth and the $n+1$ rf pulse as $\Phi(n)$. We make $\Phi(n)$ to vary from one TR to another so that it is a function of n. We seek a set of phase values $\{\Phi(n)\}$ such that in steady state there is cancellation of transverse magnetization prior to *all* rf pulses. The same phase values $\{\Phi(n)\}$ must be applied to all the spins in the selected slice or volume to ensure that cancellation of magnetization is achieved for all the excited spins. This means that $\Phi(n)$ cannot be varied by using gradients with variable amplitudes because if such gradients are applied, spins at different locations within the image will experience different phase values, resulting in good cancellation in one part of the image and no cancellation in another (*10*). Position-dependent phase shifts can be avoided if $\Phi(n)$ is varied by changing the frequency of the rf synthesizer and resetting it, as explained in the Appendix. With this procedure all the spins within the selected slice or volume experience the same phase shift.

This method of eliminating coherent transverse magnetization by phase shifts poses two problems: (a) The amplitude of the magnetization components depends on E_1, E_2, and the rf tip angle. A particular set of phase values $\{\Phi(n)\}$ might cancel transverse magnetization only over a limited range of these variables. Therefore, optimization of $\{\Phi(n)\}$ is needed to achieve maximum cancellation of magnetization over the desired range of E_1, E_2, and rf tip angles. (b) Whenever the transverse magnetization is not cancelled perfectly, variations of $\Phi(n)$ from one TR to another might cause fluctuations in the measured signal. Such fluctuations cause image blurring, ghosts, and noise in the phase encoding direction. Clearly, this problem can be solved by choosing $\{\Phi(n)\}$ in such a way that the signal remains stable for arbitrary E_1, E_2, and rf tip angle, even though $\Phi(n)$ is varying.

Choosing $\{\Phi(n)\}$ for Effective Spoiling

Suppose that the phase $\Phi(n)$ for a spin at location $\mathbf{r}$ is given by

$$\Phi(n)=\gamma\mathbf{r}\cdot\int_0^{TR}\mathbf{G}(t)dt+\psi(n)\equiv\Phi(\mathbf{r})+\psi(n), \qquad [5]$$

where $\Phi(\mathbf{r})$ is defined by Eq. [4] and is the same for all TR. The phase $\psi(n)$, which is applied by changing the frequency of the synthesizer and resetting it, is the same for all the spins in the selected slice but it changes from one TR to another.

Since $\Phi(\mathbf{r})$ in Eq. [5] is the same for all TR, the position-dependent phase of all magnetization components is $k\cdot\Phi(\mathbf{r})$, where k is an integer. As explained before, only magnetization components with $k=0$ contribute to the measured signal. The effect of $\psi(n)$ in Eq. [5] is to add a phase shift to each component, which depends on the trajectory through which it evolves and the values of $\{\psi(n)\}$. These values must be chosen so that the magnetization components with $k=0$ acquire different phases and cancel each other.

Consider the train of rf pulses shown in Fig. 1, in which TR is shorter than T_2. We focus attention on pulse P_n and assume that steady state has already been attained before P_n is applied, i.e., $(n-1)\mathrm{TR} \gg 3T_1$. The phase $\Phi(n)$ which accumulates during the TR interval subsequent to pulse P_n is given by Eq. [5]. The objective is to find values for $\psi(n)$ such that the sampled NMR signal remains the same throughout the scan for any given E_1, E_2, and rf tip angle.

From the discussion of the example in Fig. 3, it follows that the phase of any magnetization component prior to pulse P_n can be written in the form

$$\text{phase} = \sum_k \Phi(n-k) - \sum_j \Phi(n-j). \qquad [6]$$

The different terms in the sums of Eq. [6] depend on the trajectory of the component. The number of terms with negative sign depends on the number of times the phase of that trajectory was inverted by the rf pulses. For all components with zero phase due to gradients, we have

$$\sum_k \Phi(\mathbf{r}) - \sum_j \Phi(\mathbf{r}) = \Phi(\mathbf{r})(K-J) = 0, \qquad [7]$$

where K and J are the number of terms in the first and second sum of Eq. [6], respectively. The number of positive and negative phase terms in Eq. [7] must be the same for any component that contributes to the signal. Therefore, the phase of these components can be written as

$$\text{phase} = \sum [\Phi(n-k) - \Phi(n-j)]. \qquad [8]$$

For example, the phase of magnetization components 1, 2, and 3 in Fig. 3 are given by $\phi(n-1) + \phi(n-2) - \phi(n-3) - \phi(n-4)$, $\phi(n-1) - \phi(n-3)$, and $\phi(n-2) + \phi(n-1)$, respectively. Only components 1 and 2 have the same number of positive and negative phase terms, because their phase due to gradients is zero.

We want to find a set of Φ's so that Eq. [8] is independent of n for any *arbitrary* magnetization component with zero phase due to gradients prior to pulse P_n. This requirement would ensure that the steady-state magnetization remains constant throughout the scan for any given value of E_1, E_2, and rf tip angle. Therefore, Eq. [8] must be independent of n for arbitrary k and j, which can be true only if every term of the sum satisfies the relationship

$$\Phi(n-k) - \Phi(n-j) = \text{independent of } n \qquad [9]$$

for arbitrary n, k, and j. Because $\Phi(\mathbf{r})$ in Eq. [5] is the same for all rf pulses, Eq. [9] can be written as

$$\psi(n-k) - \psi(n-j) = \text{independent of } n. \qquad [10]$$

This can be fulfilled if, and only if,

$$\psi(n) = n\psi_A + \psi_B, \qquad [11]$$

where ψ_A and ψ_B are arbitrary constants. If Eq. [11] is satisfied an artifact-free image will result. That is, the steady-state magnetization remains constant throughout the scan for any given E_1, E_2, and tip angle only if the phase $\psi(n)$ is linearly incremented

by ψ_A radians in every TR interval. Note that the value selected for ψ_B affects only the total phase of the final image, and because only the magnitude of the image is displayed, the value of ψ_B is unimportant. However computer simulations in the next section show how the image contrast depends on ψ_A.

The constraint imposed by Eq. [7] applies only when $\mathbf{m}_0$, defined by Eq. [4], is large. When m_0 is small or zero, *any* magnetization component prior to P_n will contribute to the sampled signal. However, the phase in Eq. [6] must be independent of n for arbitrary n, k, and j. This can be fulfilled only if each Φ is the same for all n. In this case both longitudinal and transverse magnetization reach steady state, resulting in a refocused SSFP image. Therefore, effective spoiling can be achieved only if $\mathbf{m}_0$ is large enough.

The technique described in this paper can be implemented by using the pulse sequence of Fig. 4. Two phase encoding gradient lobes with opposite polarity and equal amplitudes must be used, so that the total phase accumulated due to gradients in each TR is the same, as required by Eq. [5]. The synthesizer frequency is changed at time t_1, after the signal has been sampled. The synthesizer is reset at time t_2, after time τ has elapsed, and a phase ψ has been added to the transverse magnetization. In each TR the frequency jump of the synthesizer is increased so that the phase $\psi(n)$ is incremented according to Eq. [11].

This spoiling technique can be implemented in three-dimensional scans by adding two phase encoding gradient lobes with opposite polarity and equal amplitudes in the slice select direction.

Computer Simulations

An optimum value of ψ_A must be selected, such that a cancellation of transverse magnetization is achieved over a wide range of values of E_1, E_2, and tip angle. We

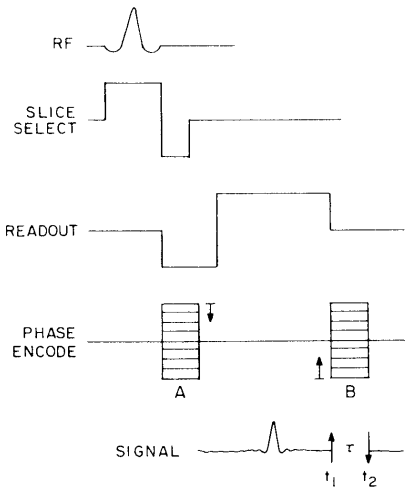

FIG. 4. Diagram of a pulse sequence which can be used to implement the described spoiling method. Phase is added to the transverse magnetization by changing the frequency of the synthesizer at time t_1, and resetting it at time t_2. This phase is incremented by advancing to a progressively higher frequency at t_1 in each TR.

developed computer simulations to verify the theoretical predictions and to choose the optimum value of ψ_A. The Bloch equations were solved to follow the time evolution of the magnetization of an isochromat every 10 μs in response to the pulses in Fig. 4. The rf pulses were nonselective, to simplify the calculations. Magnetic field gradients were included by calculating and adding the time evolution of 200 isochromats. The precessional frequencies of these 200 isochromats were chosen so as to give the phases $\Phi(\mathbf{r})$, defined in Eq. [4a], a uniform distribution over the entire range of 360°.

The signal S^+ immediately after each rf excitation in a train of pulses was calculated in the presence of the gradients shown in Fig. 4 for a variety of phase shifts $\psi(n)$. In each TR the phase shift $\psi(n)$ was incremented according to Eq. [11]. The result is presented in Fig. 5. It is seen that for any value of phase increment ψ_A, S^+ stabilizes after about $4T_1$ s (i.e., 160 rf pulses) and remains constant, as predicted by the theory. The magnitude of the steady-state signal depends on the phase increment ψ_A. In Fig. 6, S^+ is calculated for the case where $\psi(n)$ changes randomly in the range 0° to 360°. Here S^+ fluctuates randomly from one TR to another, and would lead to severe artifacts in the phase encoding direction of the image.

In order to find the optimum value of ψ_A, the steady-state signal S_{ss}^+ was calculated as a function of ψ_A and plotted in Figs. 7a and 7b. Peaks in the amplitude of S_{ss}^+ are observed for certain values of phase increment. Crawley *et al.* (*10*) and Sekihara (*19*) pointed out that these peaks occur when ψ_A is equal to $360°/m$, where m is an integer, as a result of incomplete cancellation of transverse magnetization prior to each rf pulse. The phase increment ψ_A that causes full cancellation of transverse magnetization prior to the rf pulses is the one whose steady-state signal intensity is identical to the FLASH signal given by Eq. [2]. The dashed line in Figs. 7a and 7b corresponds to the FLASH signal. The calculated signal S_{ss}^+ is very close to the FLASH signal for all the relaxation times and rf tip angles shown, when $\psi_A = 117°$ or $\psi_A = 123°$, as indicated by the arrows. We repeated the calculation of the steady-state signal S_{ss}^+ for T_1/TR

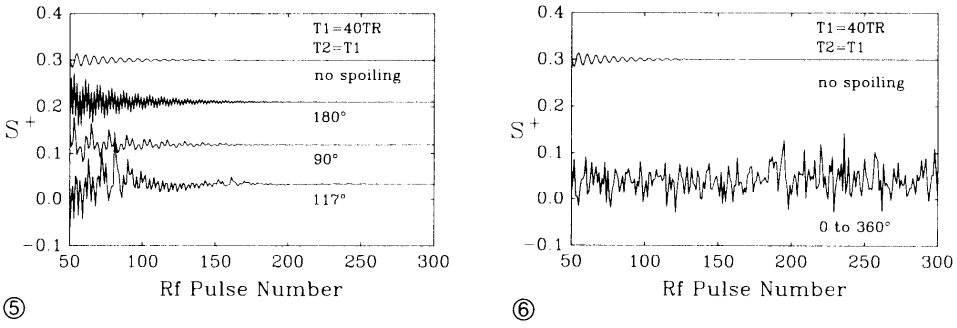

FIG. 5. The calculated S^+ signal immediately after each rf excitation in a train of pulses in the presence of gradients (Fig. 4). In each TR a phase shift $\psi(n)$ was applied, as explained in Fig. 4, and incremented linearly. Computer simulations are shown for phase increments of 180°, 90°, and 117°. The rf tip angle was 60°.

FIG. 6. Computer simulations of S^+ immediately after each rf excitation in a train of pulses similar to the method of Fig. 5. The phase shift $\psi(n)$ changed randomly between 0° and 360°. The rf tip angle was 60°.

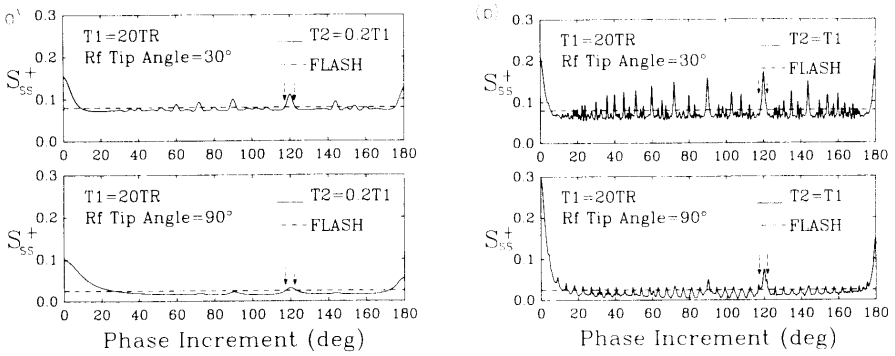

FIG. 7. Simulations of the steady-state signal S_{ss}^{+} arising from the pulse sequence in Fig. 4 as a function of the phase shift increment ψ_A. Steady-state conditions were ensured by applying the train of rf pulses for $4T_1$ before S_{ss}^{+} was calculated. A phase increment of 117° or 123°, indicated by the arrows, results in a steady-state signal which is approximately equal to the FLASH signal.

in the range 10 to 40, and for T_2/T_1 in the range 0.1 to 1, since these encompass the range of values encountered clinically. In each calculation the rf tip angle was varied from 0° to 90°. We found that S_{ss}^{+} is consistently very close to the theoretical FLASH signal only when ψ_A is 117° or 123°. This is demonstrated in Fig. 8 for a range of parameters.

EXPERIMENTS

Theoretical predictions from the previous sections were validated by acquiring images of uniform phantoms and human subjects. The imaging pulse sequence was developed

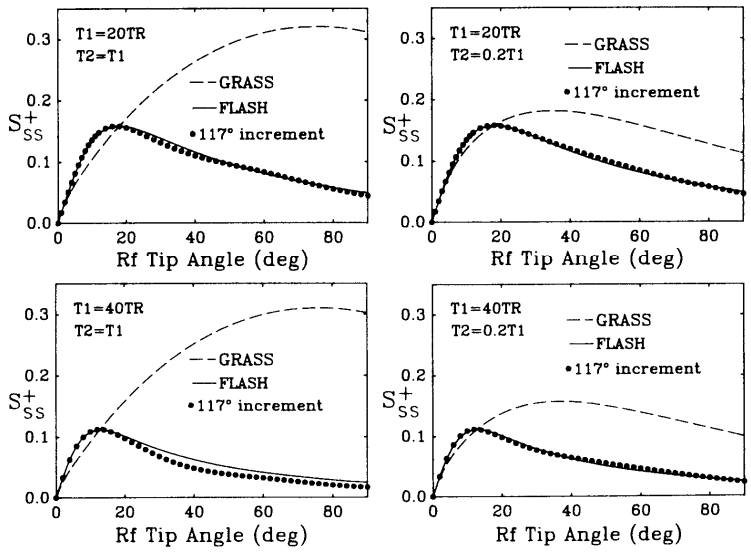

FIG. 8. Simulations of S_{ss}^{+} with spoiling by phase shifts that increased linearly by 117° compared to predictions of S_{ss}^{+} for FLASH and GRASS (*4*). The rf pulses were applied for $4T_1$ before S_{ss}^{+} was calculated.

on a Siemens Magnetom 1.0-T MRI unit. Spoiling was implemented by using rf pulses of different phase, as explained in the Appendix. The measured data were phase-shifted to compensate for each rf pulse and were then reconstructed into images using the fast Fourier transform.

Various patterns for spoiling were evaluated on uniform phantoms. Figure 9a illustrates spoiling by the phase encoding gradient alone, without additional phase shifts. Lobe B of the phase encoding gradient shown in Fig. 4 was removed for this image. The bright horizontal band occurs at the center of the phase encoding direction, where the phase encoding gradient is too weak to spoil the transverse magnetization (*10*). The pulse sequence shown in Fig. 4, including lobe B of the phase encoding gradient, was used for the experiments to evaluate spoiling by phase shifts. In Fig. 9b a random phase shift between 0° to 360° was applied in each TR interval, producing conspicuous ghosts in the phase encoding direction. Appearance of these ghosts is not surprising, given the results of Fig. 6. The phase shifts for Fig. 9c were incremented linearly by 117°. The image is artifact-free and of uniform intensity as predicted by Eq. [11].

This observation extends to the images of a human subject (Fig. 10). It is verified that phase shifts incremented linearly by 117° spoil the transverse magnetization without altering the contrast between gray and white matter and without producing any artifacts.

DISCUSSION

We have presented a method to eliminate steady-state transverse magnetization prior to each rf excitation in pulse sequences where TR $\ll T_2$. An artifact-free image

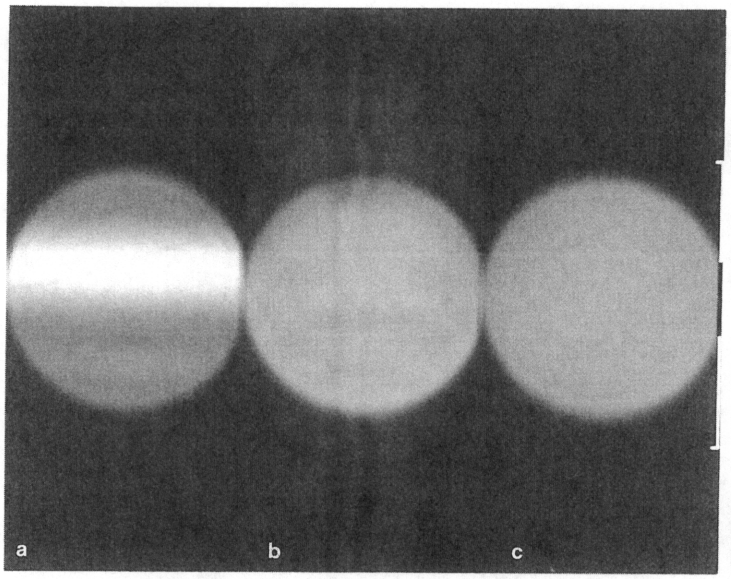

FIG. 9. Three images of a uniform phantom that demonstrate spoiling. The conventional linearly incremented phase encoding gradient, without a rephasing lobe, was applied for image (a). Random phase shifts between 0° and 360° were applied for image (b). The phase shifts for image (c) increased linearly by 117°. The T_1 and T_2 of the phantom were approximately 400 ms each. The rf tip angle was 60° and TR was 25 ms.

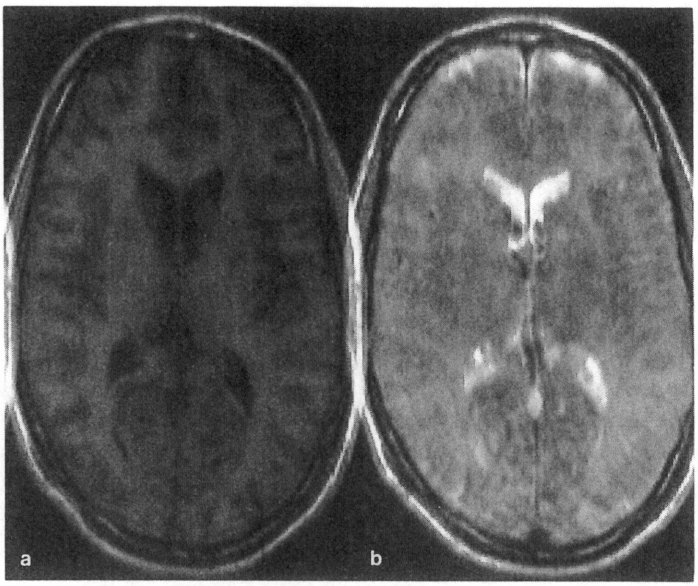

FIG. 10. Images of the human head obtained (b) without changing the frequency of the synthesizer at time t_1, resulting in a refocused SSFP image with bright cerebrospinal fluid, and (a) with a linearly incremented phase shift, resulting in high T_1 contrast and demonstration that effective spoiling was achieved. TR was 33 ms and the rf tip angle was 60°. The images are from a three-dimensional acquisition, with the first phase encoding direction mediolateral and the second phase encoding direction anterosuperior.

with high T_1 contrast can be obtained when a phase shift that is incremented linearly during each TR interval is applied. When this phase increment is 117°, the steady-state signals agree closely with those of FLASH, indicating that complete spoiling has been achieved. Consequently, image contrast becomes independent of T_2. From our computer simulations it is apparent that almost all other values for the phase increment fail to remove the T_2 dependence. The motivation to eliminate this dependence stems from the following consideration. Tissues with longer T_1 values generally also have longer T_2 values (*20*). When comparing two tissues, the steady-state signal S_{ss}^{+} from the one with longer T_1 will be weakened because of slower T_1 recovery but will be enhanced by the longer T_2 since it produces a larger refocused signal. The net effect is that the contrast between the two tissues is reduced. Hence, elimination of the T_2 dependence leads to improved contrast.

We have also shown that the steady-state transverse magnetization cannot be spoiled by applying large gradient pulses of constant amplitude during each TR interval. While images showing evidence of spoiling have been produced using this technique (*14*), it should be recognized that such spoiling is caused by the random Brownian motion of the spins in the presence of large gradient pulses (*21*). Consequently, the contrast between tissues becomes dependent on the diffusion coefficient.

CONCLUSION

Our analysis shows that artifact-free images with true spoiling of transverse magnetization can be obtained only if the following conditions are fulfilled: (a) In each

TR interval a phase $\psi(n)$ is added to the transverse magnetization and $\psi(n)$ is linearly incremented by ψ_A radians in each TR. The same phase value, $\psi(n)$, must be applied to all the spins in the selected slice or volume. (b) ψ_A must be different than $360°/m$, where m is an integer. If ψ_A is set to 117° or 123°, adequate cancellation of transverse magnetization can be achieved for all values of T_1/TR and T_2/TR which are encountered clinically. (c) The value of $\mathbf{m}_0$ (defined by Eq. [4]) must be large enough so that only magnetization components with zero phase due to gradients contribute to the measured signal. (d) For each spin, the total phase due to gradients must be the same in each TR interval. Using this method images with good T_1 contrast and high signal-to-noise ratio per unit time can be obtained.

APPENDIX

The phase of the transverse magnetization can be altered by changing the frequency of the synthesizer in the spectrometer by $\Delta\nu$ Hz and then resetting it after τ s (*22*). If a phase shift of ψ radians is desired, $\Delta\nu$ and τ are set so that

$$\psi = -2\pi\Delta\nu\tau. \qquad [A1]$$

The frequency $\Delta\nu$ is incremented to increment the phase ψ according to Eq. [11]. The frequency jump and reset is carried out during every TR interval immediately after data sampling and before the next rf pulse, as shown in Fig. 5. During the first TR, $\Delta\nu$ is set to some initial value and it is incremented in subsequent TR intervals until the scan is completed. These phase shifts are accurate because $\Delta\nu$ can be set very accurately using modern synthesizers. For example, ψ can be set with an accuracy of 0.04 degrees if the accuracy of $\Delta\nu$ is 0.1 Hz and $\tau = 1$ ms. This method was originally demonstrated by Zur and Bendel (*9*).

Crawley *et al.* (*10*) proposed an alternate method to achieve the phase increments of Eq. [11]. In this case the phase of the rf pulses is incremented, while the frequency of the synthesizer remains unchanged. The phase shift $\Theta(n)$ applied to the nth rf pulse P_n is given by

$$\Theta(n) = \sum_{j=0}^{n-1} j\psi_A, \qquad [A2]$$

where ψ_A is the phase increment in Eq. [11], and j is an integer. From Eq. [A2] we obtain

$$\Theta(n+1) - \Theta(n) = n\psi_A. \qquad [A3]$$

The phase of the received signal, which is sampled immediately after pulse P_n, must also be shifted by $\Theta(n)$. The resulting signal is analyzed by transforming to a rotating frame where the phase of the rf pulses and the receiver is constant in time. We call this the rf rotating frame. In the laboratory frame the precession frequency of the transverse magnetization is constant. Equation [A3] shows that the phase difference which accumulates between the transverse magnetization and the rf rotating frame in the time interval between rf pulses P_n and P_{n+1} is $n\psi_A$. Therefore, the signal measured in this rf rotating frame is identical to the signal obtained by incrementing the frequency of the synthesizer. It is cumbersome and less accurate to vary the phase of the rf pulses

because any small systematic errors in the phase of the rf pulse or the receiver accumulate as n increases. However, such errors might be circumvented by the use of modern digital transceiver technology. This alternative can be used if the frequency of the synthesizer cannot be varied.

ACKNOWLEDGMENTS

This research was supported by the Toshiba Corporation (Y.Z. and L.J.N.). M.L.W. was supported in part by a grant from the Division of Research Resources, National Institutes of Health (SO7-RR05598).

REFERENCES

1. A. HAASE, J. FRAHM, D. MATTHEI, W. HÄNICKE, AND K. D. MERBOLDT, *J. Magn. Reson.* **67,** 258 (1986).
2. A. OPPELT, R. GRAUMANN, H. BARFUSS, H. FISCHER, W. HARTL, AND W. SCHAJOR, *Electromedica* **54,** 15 (1986).
3. M. L. GYNGELL, N. D. PALMER, AND L. M. EASTWOOD, "S.M.R.M. Book of Abstracts, Montreal, 1986," p. 666.
4. J. A. UTZ, R. J. HERFKENS, G. GLOVER, AND N. PELC, *Magn. Reson. Imaging* **4,** 106 (1986).
5. H. Y. CARR, *Phys. Rev.* **112,** 1693 (1958).
6. R. FREEMAN AND H. D. W. HILL, *J. Magn. Reson.* **4,** 366 (1971).
7. Y. ZUR, S. STOKAR, AND P. BENDEL, *Magn. Reson. Med.* **6,** 175 (1988).
8. W. A. EDELSTEIN, P. A. BOTTOMLEY, H. R. HART, AND L. S. SMITH, *J. Comput. Assist. Tomogr.* **7,** 391 (1983).
9. Y. ZUR AND P. BENDEL, "S.M.R.M. Book of Abstracts, New York, 1987," p. 440.
10. A. P. CRAWLEY, M. L. WOOD, AND R. M. HENKELMAN, *Magn. Reson. Med.* **8,** 248 (1988).
11. J. FRAHM, W. HÄNICKE, AND K. D. MERBOLDT, *J. Magn. Reson.* **72,** 307 (1987).
12. L. DARRASSE, L. MAO, AND H. SAINT-JAMES, "S.M.R.M. Book of Abstracts, Montreal, 1986," p. 944.
13. M. L. WOOD, M. SILVER, AND V. M. RUNGE, *Magn. Reson. Imaging* **5,** 455 (1987).
14. M. L. WOOD AND V. M. RUNGE, *Med. Phys.* **15**(6), 825 (1988).
15. R. R. ERNST, G. BODENHAUSEN, AND A. WOKAUN, "Principles of Magnetic Resonance in One and Two Dimensions," p. 124, Clarendon Press, Oxford, 1987.
16. D. E. WOESSNER, *J. Chem. Phys.* **34,** 2057 (1961); R. KAISER, E. BERTHOLDI, AND R. R. ERNST, *J. Chem. Phys.* **60,** 2966 (1974).
17. J. HENNIG, *J. Magn. Reson.* **78,** 397 (1988).
18. Y. ZUR AND S. STOKAR, *J. Magn. Reson* **71,** 212 (1987).
19. K. SEKIHARA, *IEEE Trans. Med. Imaging* **MI-6,** 157 (1987).
20. P. BENDEL, *Magn. Reson. Med.* **5,** 366 (1987).
21. K. D. MERBOLDT, W. HÄNICKE, M. L. GYNGELL, J. FRAHM, AND H. BRUHN, *Magn. Reson. Med.* **12,** 198 (1989).
22. Y. ZUR, M. L. WOOD, AND L. J. NEURINGER, *Magn. Reson. Med.* **16,** 444 (1990).